Earthquakes Detectability of KUT Infrasound Sensor Network During 2019

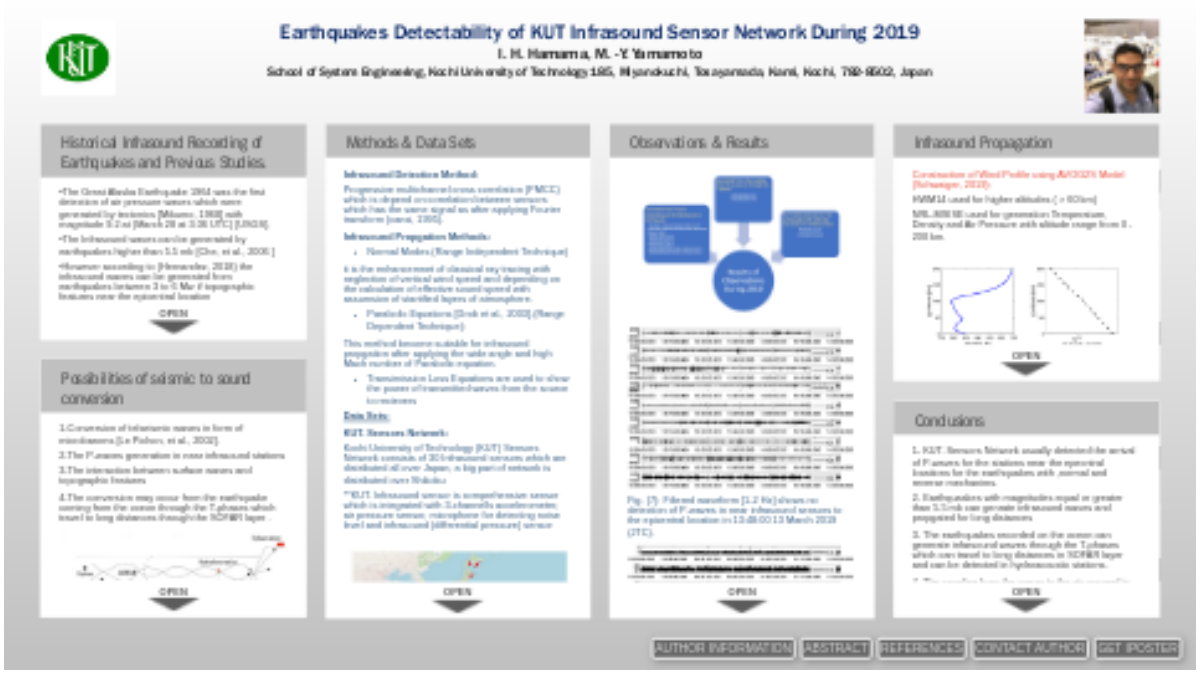

I. H. Hamama, M. -Y. Yamamoto

School of System Engineering, Kochi University of Technology 185, Miyanokuchi, Tosayamada, Kami, Kochi, 782-8502, Japan

PRESENTED AT:

JpGU - AGU Joint Meeting 2020

For a Borderless World of Geoscience

Japan Geoscience Union, American Geophysical Union

HISTORICAL INFRASOUND RECORDING OF EARTHQUAKES AND PREVIOUS STUDIES.

•The Great Alaska Earthquake 1964 was the first detection of air pressure waves which were generated by tectonics [Mikumo, 1968] with magnitude 9.2 at (March 28 at 3:36 UTC) [USGS].

•The Infrasound waves can be generated by earthquakes higher than 5.5 mb [Che, et al., 2006]

•However according to (Hernandez, 2018) the infrasound waves can be generated from earthquakes between 3 to 6 Mw if topographic features near the epicentral location

•In the Local earthquakes P-waves can be detected in Infrasound sensors [Mutschlecner, 2005]

Fig. (1): Historical picture for dustriction of the great Alaska earthquake at 1964.
Ref.: https://www.theatlantic.com/photo/2014/05/1964-alaskas-good-friday-earthquake/100746/
(https://www.theatlantic.com/photo/2014/05/1964-alaskas-good-friday-earthquake/100746/)

POSSIBILITIES OF SEISMIC TO SOUND CONVERSION

1-Conversion of telseismic waves in form of microbaroms [Le Pichon, et al., 2002].

2-The P-waves generation in near infrasound stations

3-The interaction between surface waves and topographic features

4-The conversion may occur from the earthquake coming from the oceon through the T-phases which travel to long distances through the SOFAR layer .

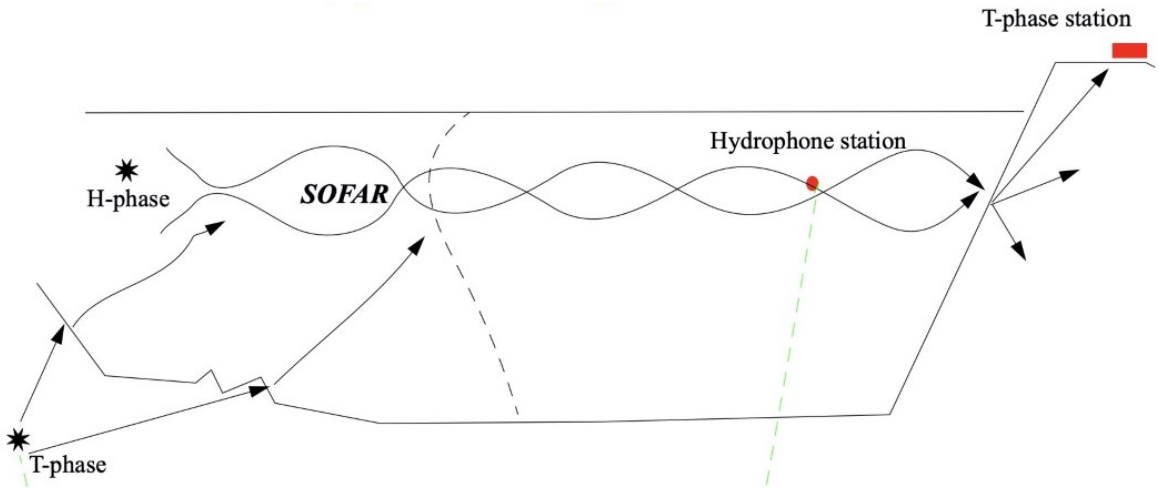

Fig. (2): Illustartion of the transmission of T-phase through the SOFAR layer on the oceon from the source to the reciever

Seismicity of Southern of Japan [2000-2020]

- 1900 Earthquakes recorded in the last 20 years in southern part of Japan around Shikoku Island with different mechanism
- The seismic activity was clearly low before the great Tonankai earthquake in 1946[Okano et al., 1979].
- According to (Shelly, et, al., 2008),Shikoku Island charactrized by low-frequancy earthquakes and the tremors are resulted from slow shear slip which can make P-waves not detectable

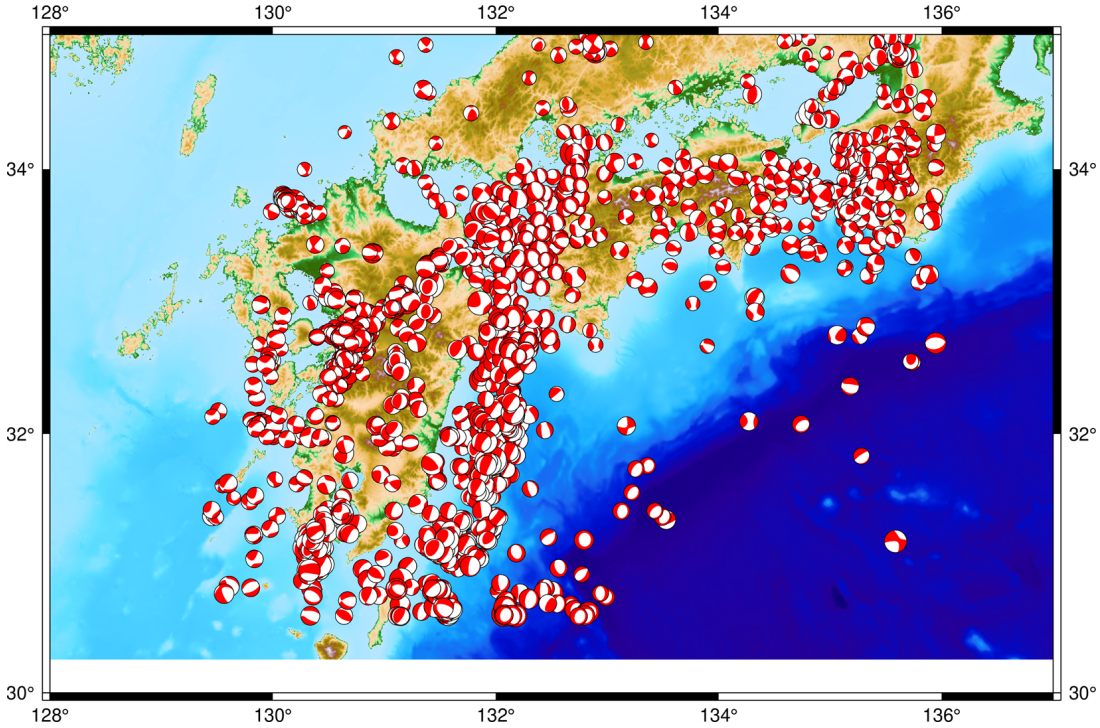

Fig. (3): The distribution of earthquakes with different mechanisms from January 2000 to January 2020 in southern of Japan

METHODS & DATA SETS

Infrasound Detection Method:

Progressive multichannel cross correlation (PMCC) which is depend on correlation between sensors which has the same signal as after applying Fourier transform (cansi, 1995).

Infrasound Propgation Methods:

- Normal Modes (Range Independent Technique)

it is the enhancemnet of classical ray tracing with neglection of vertical wind speed and depending on the calculation of effective sound speed with assumsion of startified layers of atmosphere.

- Parabolic Equations [Drob et al., 2003].(Range Dependent Technique):

This method become suitable for infrasound propgation after applying the wide angle and high Mach number of Parabolic equation.

- Transimission Loss Equations are used to show the power of transmitted waves from the source to recievers

Data Sets:

KUT. Sensors Network:

Kochi University of Technology (KUT) Sensors Network consists of 30 Infrasound sensors which are distributed all over Japan, a big part of network is distributed over Shikoku

**KUT. Infrasound sensor is comprehensive sensor which is integrated with 3-channells accelerometer, air pressure sensor, microphone for detecting noise level and infrasound (differential pressure) sensor

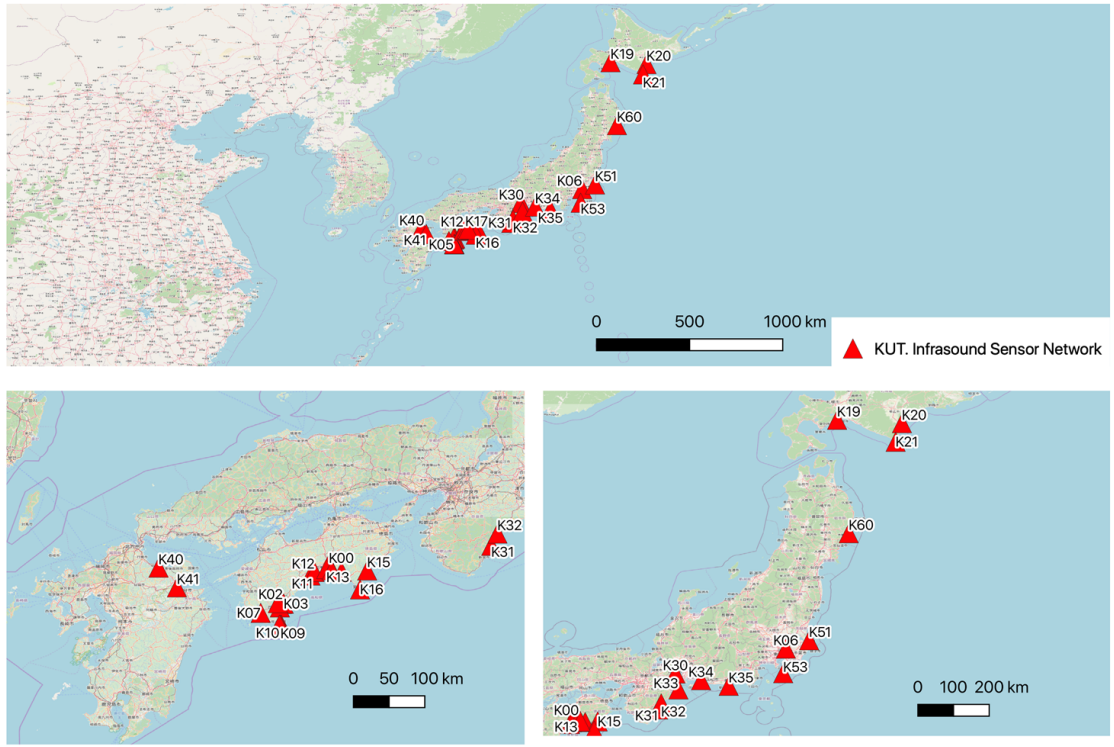

Fig. (4): The locations of KUT. Infrasound sensors which are located all over Japan.

IMS. Stations:

1- Infrasound Data: I30 JP. Infrasound station of International Monitoring System (IMS) which is consist of 6 sensors with diameter vary from 1 to 3 km

2-Hydroacoustic Data: H11N station which consist of 3 sensors N1, N2 and N3

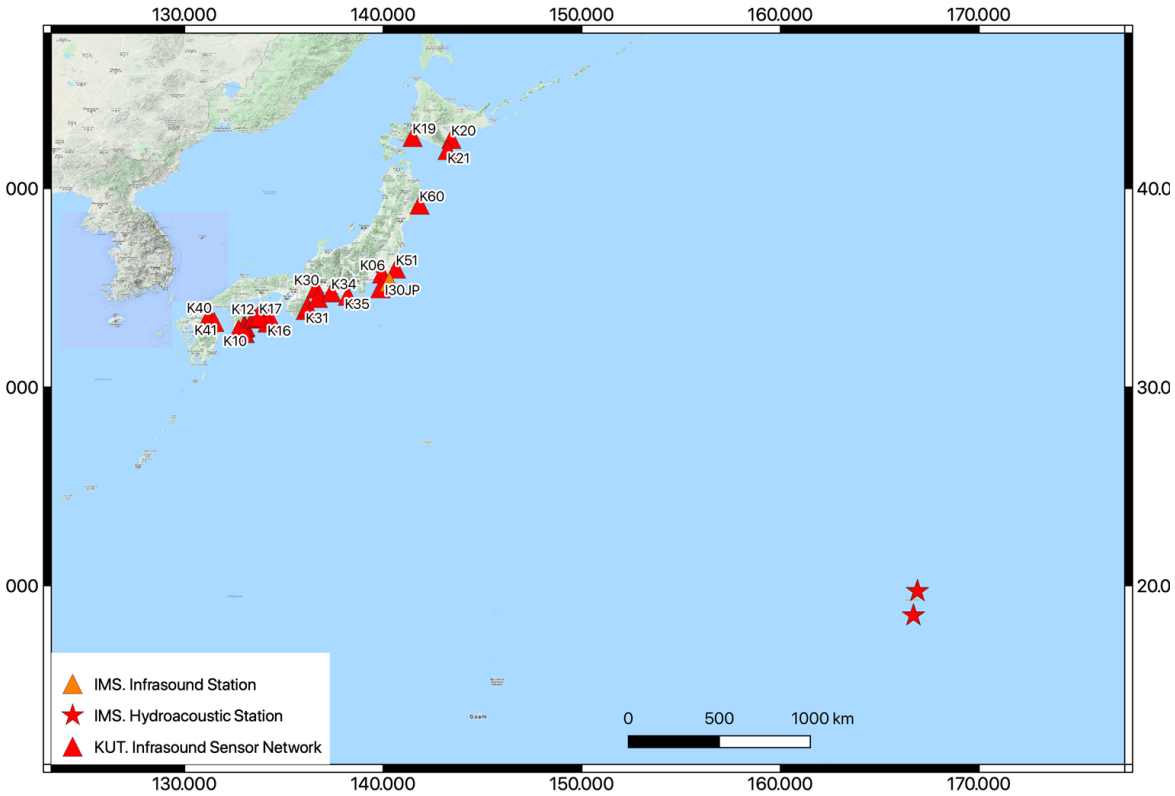

Fig. (5): All sources of data including IMS. statsion (Infrasound, Hydroacoustic)

NCEP.:

The horizontal wind speed data extracted from Reanalysis data of National Centers Environmental Prediction .

Selected Events Criteria for The Study During 2019:

1- Recorded in All Bulletins(USGS, JMA, IDC)

2- Magnitude > 4.4 mb.

3- In and around Shikoku Island.

4- Depth not exceeds 50 Km. (Shallow depth Earthquake).

Date	Event Time UTC	Mag. (mb.)	Long.	Lat.	Depth (km)	Source Mechanism
2019/03/11	06:37	4.9 mb	132.71	33.1903	38.13	Strike-Slip
2019-03/07	02:20	4.4 mb	134.79	33.3703	31.61	Reverse
2019/03/13	04:48	5.1 mb	134.91	33.801	43.05	Strike-Slip
2019/05/09	22:43	5.8 mb	131.99	31.785	25.35	Reverse
2019/05/09	23:48	6.0 mb	131.97	31.80	25.46	Reverse
2019/05/10	23:59	5.0 mb	132.29	32.6903	36.34	Normal
2019/05/12	06:07	4.7 mb	132.29	32.7053	36.66	Normal

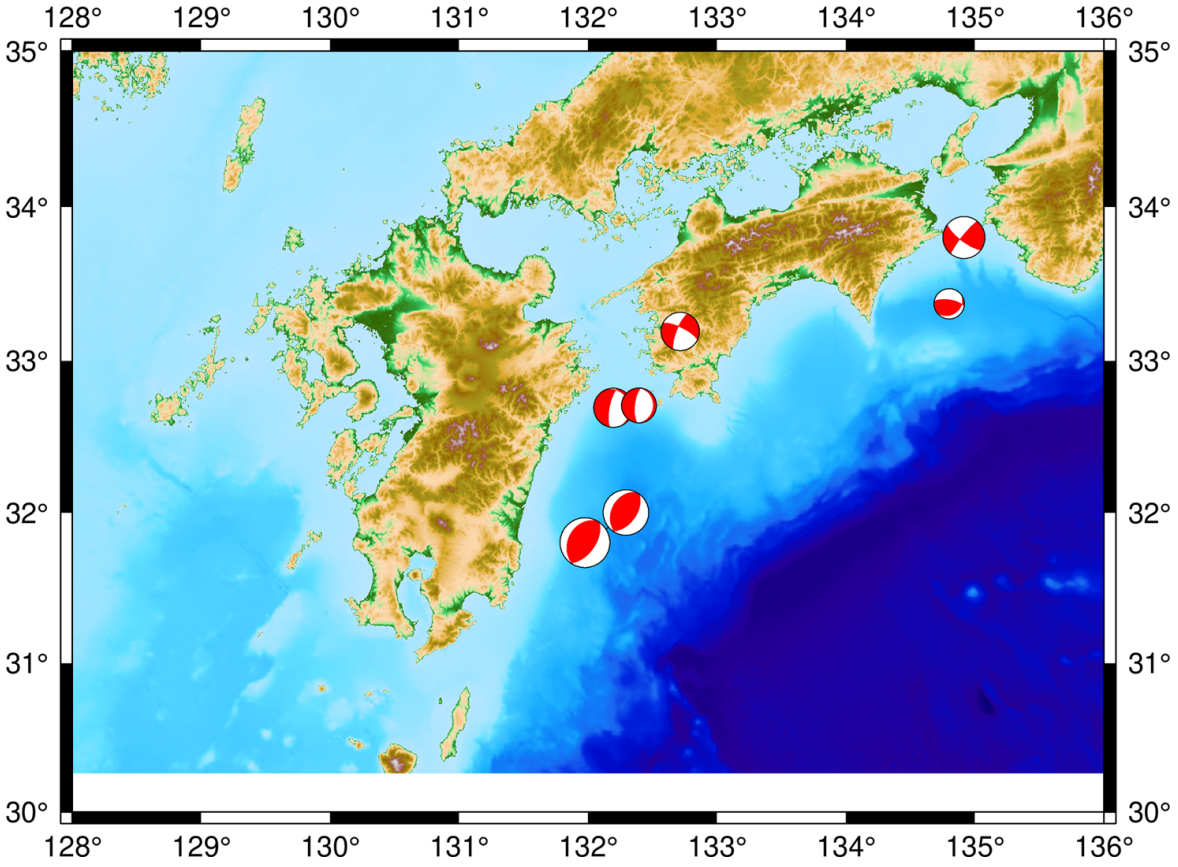

Fig. (6): The selected events in the study according to many parameters; magnitude, depth and mechanisms

OBSERVATIONS & RESULTS

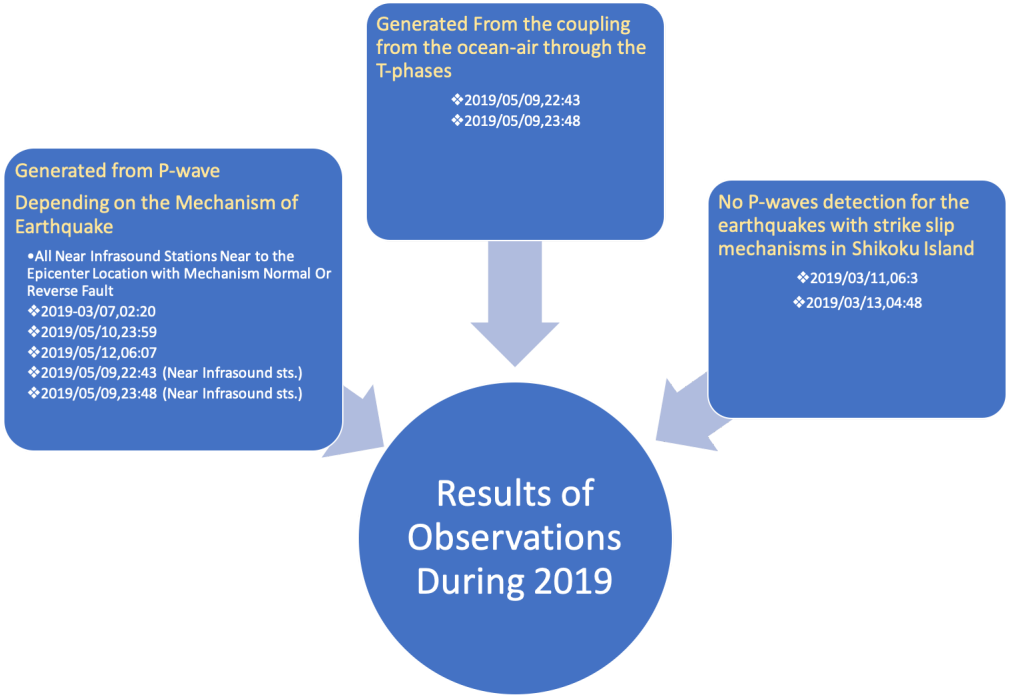

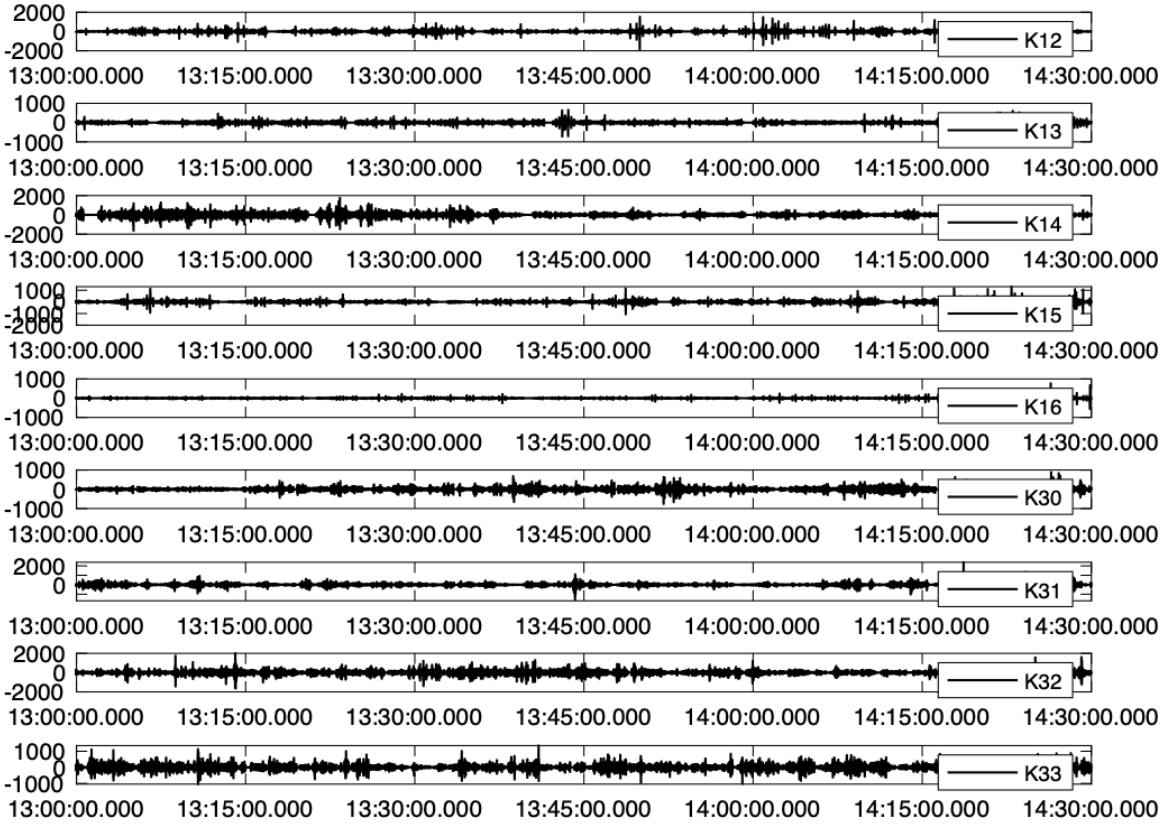
2000
0
-2000
K12
13:00:00.000
13:15:00.000
13:30:00.000
13:45:00.000
14:00:00.000
14:15:00.000
14:30:00.000
1000
0
-1000
K13
K14
K15
K16
K30
K31
K32
K33

Fig. (7): Filtered waveform [1-2 Hz] shows no detection of P-waves in near infrasound sensors to the epicentral location in 13:48:00 13 March 2019 (JTC).

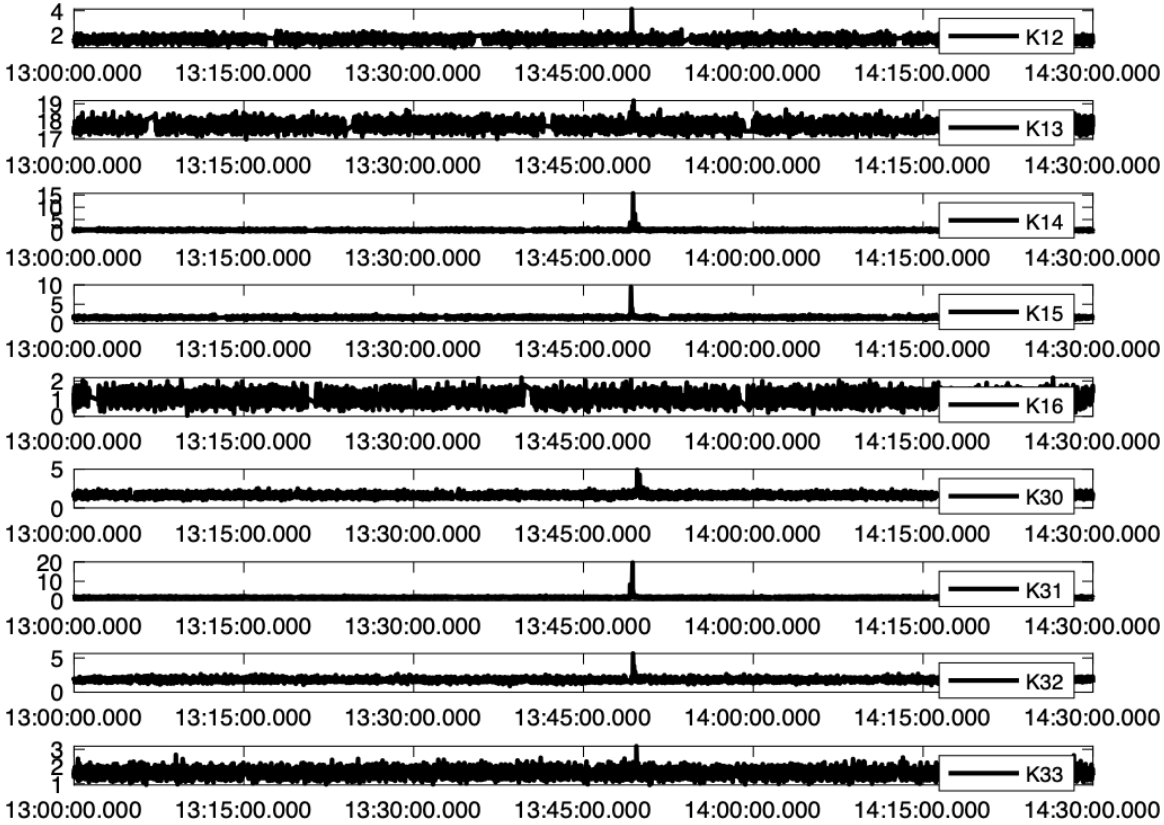

Fig. (8): Filtered acelerometter waveform [1-2 Hz] at 13:48:00 13 March 2019 (JTC).

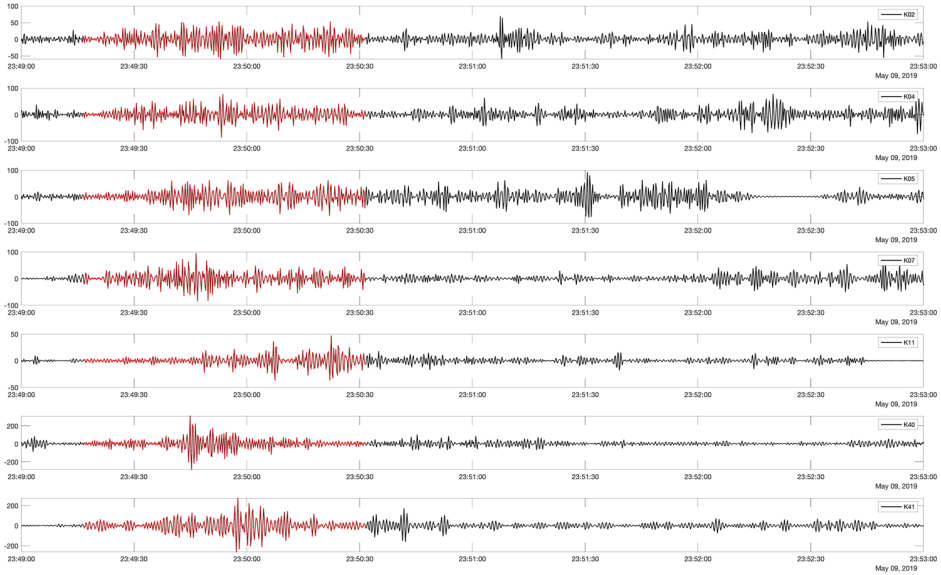

Fig. (9): Filtered [1-2 Hz] recorded P-waves of the earthquake which occurred at 23:48:00 UTC. on 09 May 2020 and well recorded in KUT. Infrasound Sensors [K02, K04, K05, K07, K11, K40, K41].

Earthquake 09, May 2019 23:48:00 UTC :

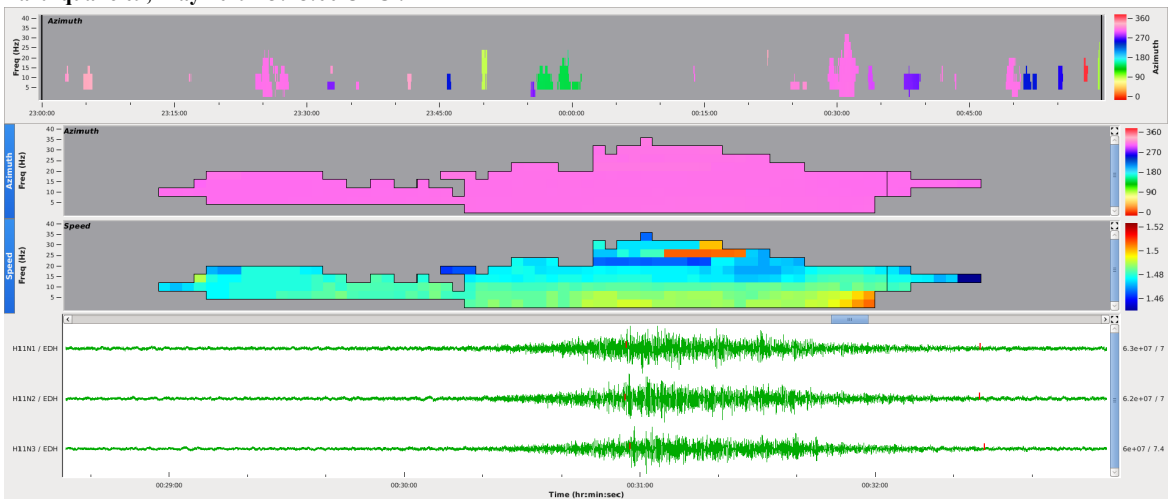

Fig. (10): Long duration T-phase waves which were generated from the main shock at 23:48:00 UTC. And were recorded at NH11 after almost 1 hour from the previous record at 00:29 to 00:32:40

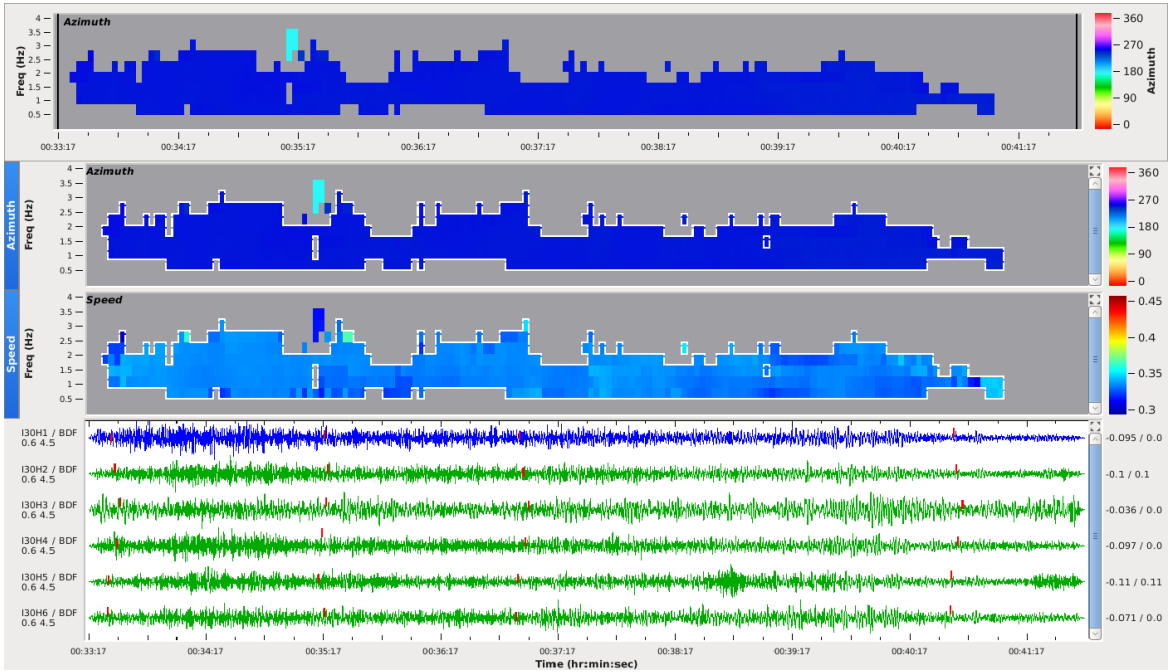

Fig. (11):Progressive multichannel cross correlation of one-hour waveform from I30 JP with window length 30 sec. and overlapping 90 at 00:31:30 UTC with back-azimuth ~ 244 degree and the frequency content range from .6 to 2.6 Hz with apparent velocity 339 m/sec

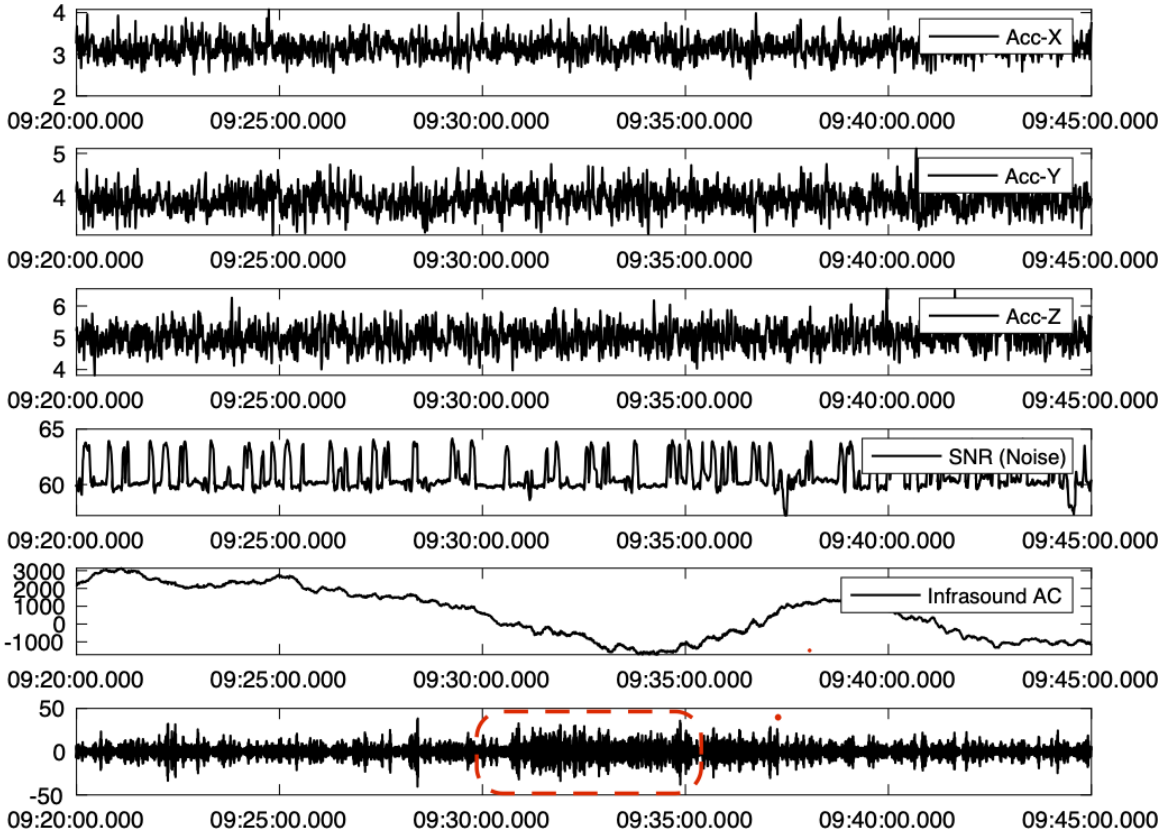

Fig. (12): K53 comprehensive sensor recording from 9:20:00 to 09:45:00 JST shows the same signal recorded in I30 JP at 9:31:00 JTC, the filtered between 1.0 to 2.0 Hz and resampled by 5 sample/sec

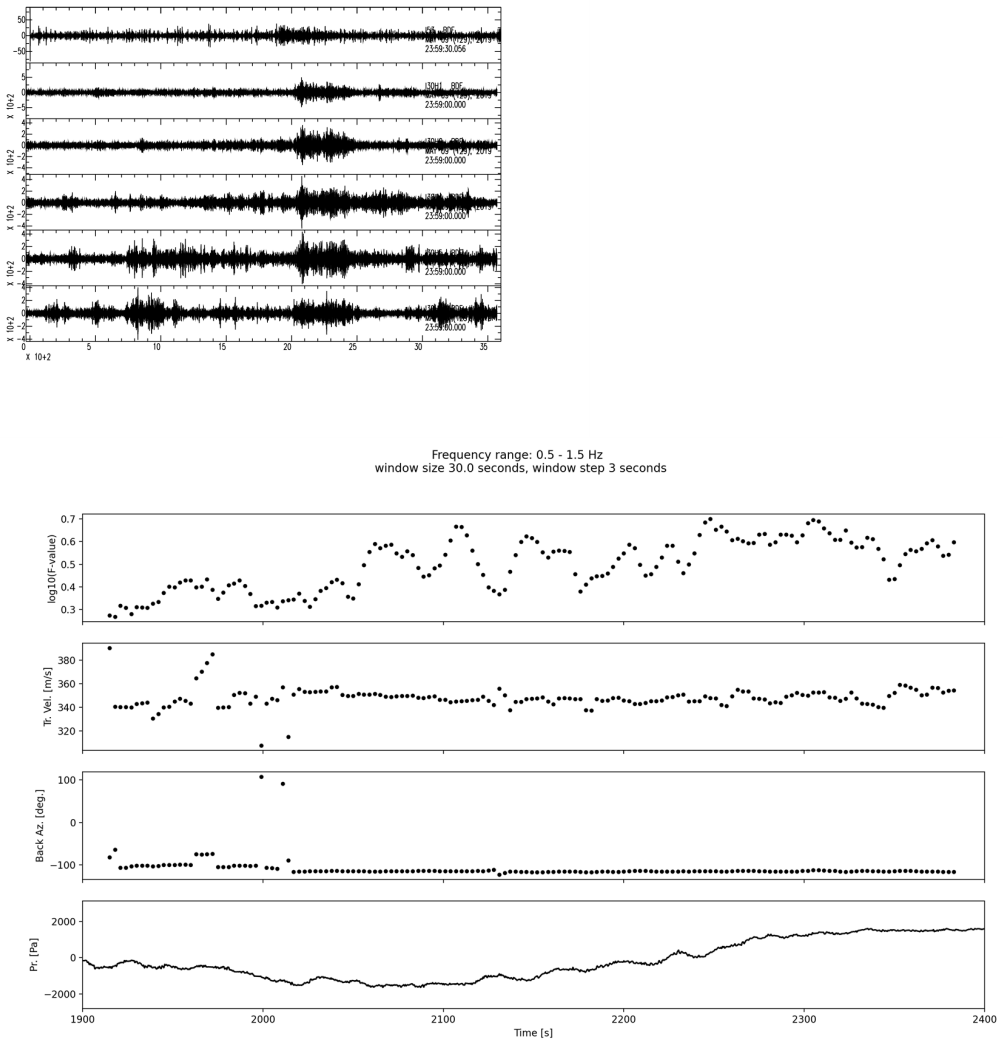

Fig. (13): Infrasonic waves recorded from I30 array and K53 together and beamforming of the sensors of I30 and single sensor of KUT. K53 for one hour 23:00 to 00:00 UTC. the F-ratio getting higher at the trace velocity ~ 340 m/sec and azimuth – 117 degree.

INFRASOUND PROPAGATION

Construction of Wind Profile using AVOG2S Model (Schwaiger, 2019):

HWM14 used for higher altitudes (> 60 km)

NRL-MSISE used for generation Temperature, Density and Air Pressure with altitude range from 0 - 200 km.

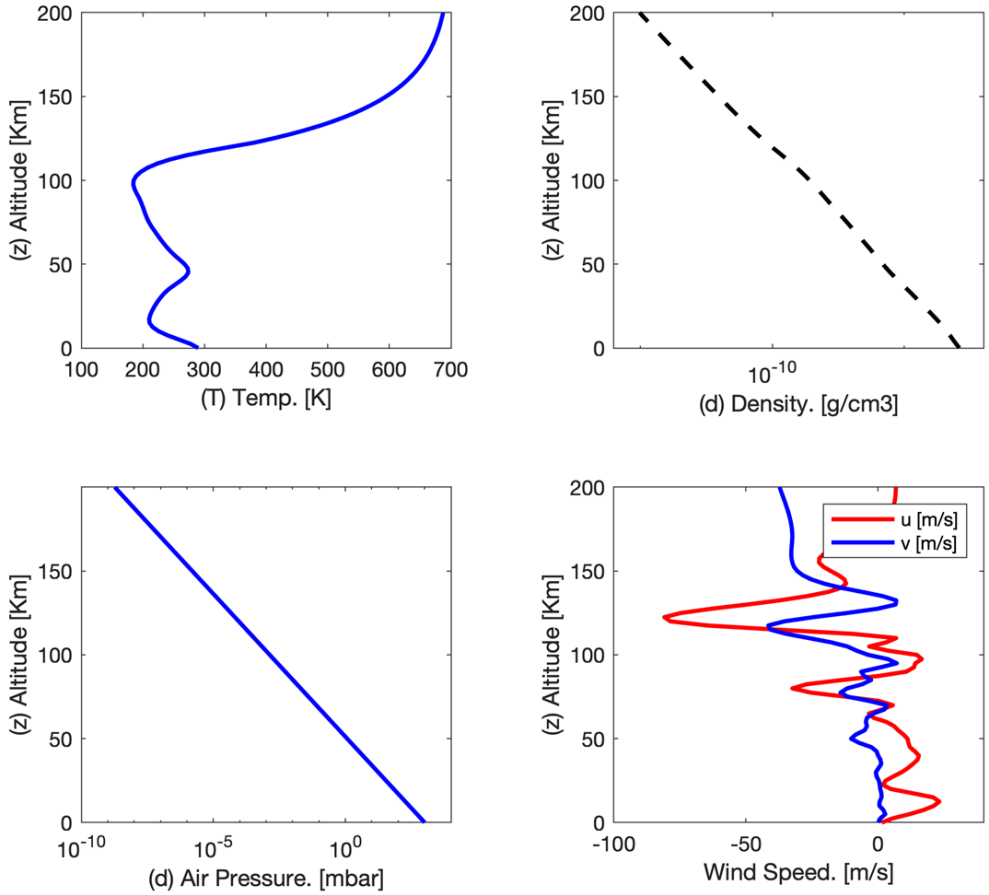

Fig. (14) : The computed temperature, density and air pressure from o to 200 km using NRL-MSISE Model,the light lower panel shows the horizontal wind speed profile which was estimated from AVOG2S model the red line refers to the zonal wind speed in m/sec and the blue line refers to the meridional sound speed in m/sec.

GeoAc.Global-Range-Independant Method applied for 3D-Raytracing:

(A)

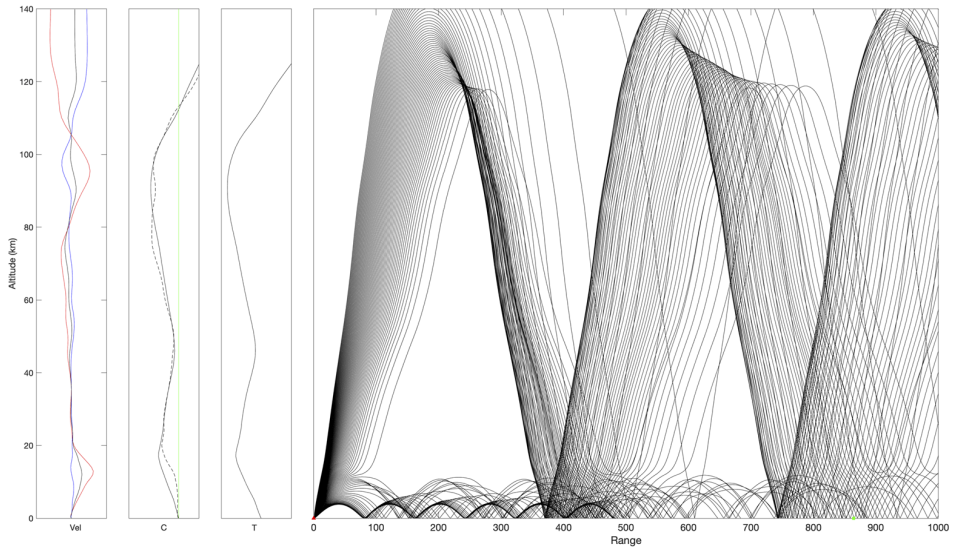

(B)

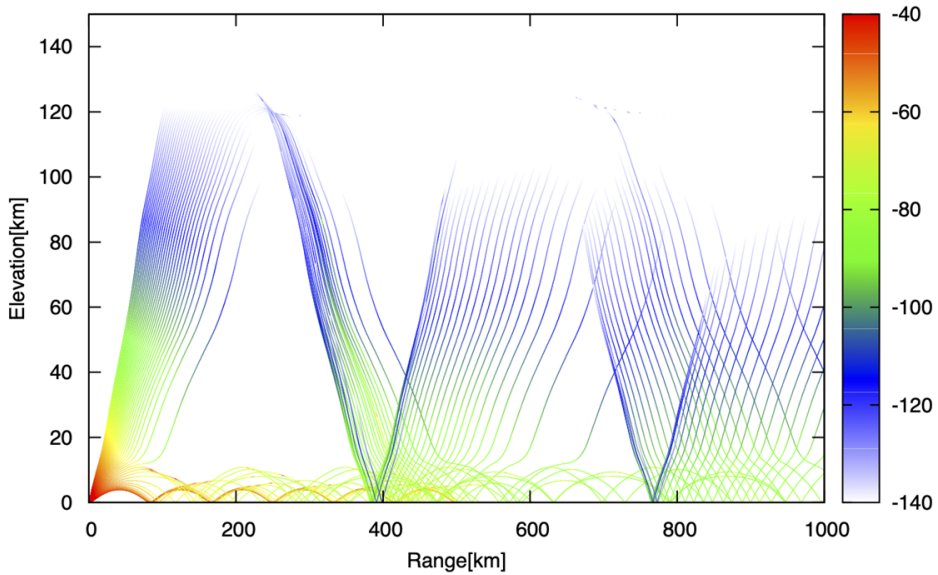

Fig. (15): The profile resulted from 3d-ray tracing using stratified propagation method, from the left represents the horizontal wind speed profile, sound speed, Temperature and the rays propagation respectively.

(B) 3d-raytracing from the epicenter location of the earthquake to range 1000 km with power of the rays in db.

Calculated Celirity:

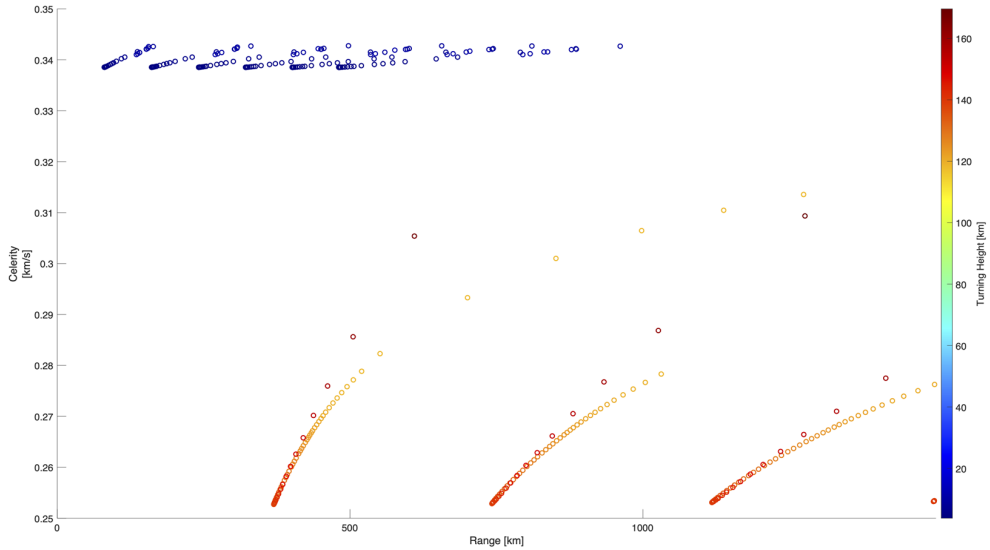

Fig. (16): Estimated celerity at range 1000 km and with altitude varying from 0 to 180 km, the blue circles refers to the tropospheric phases with celerity around 340 m/sec, the red to orange circles shows the thermosphere phases with lower celerity

Calculated Transsimision loss by Range Independent and Range Dependent Methods：

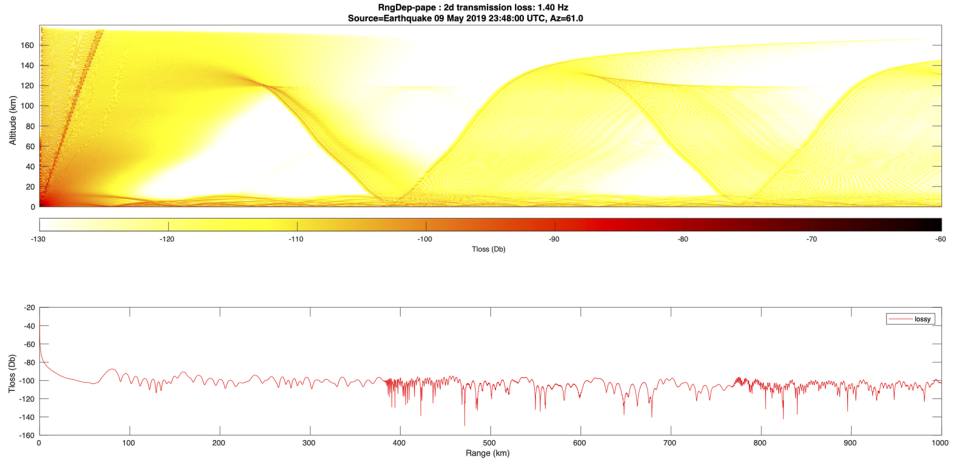
RngDep-pape : 2d transmission loss: 1.40 Hz
Source=Earthquake 09 May 2019 23:48:00 UTC, Az=61.0
Altitude (km)
Tloss (Db)
lossy
Range (km)

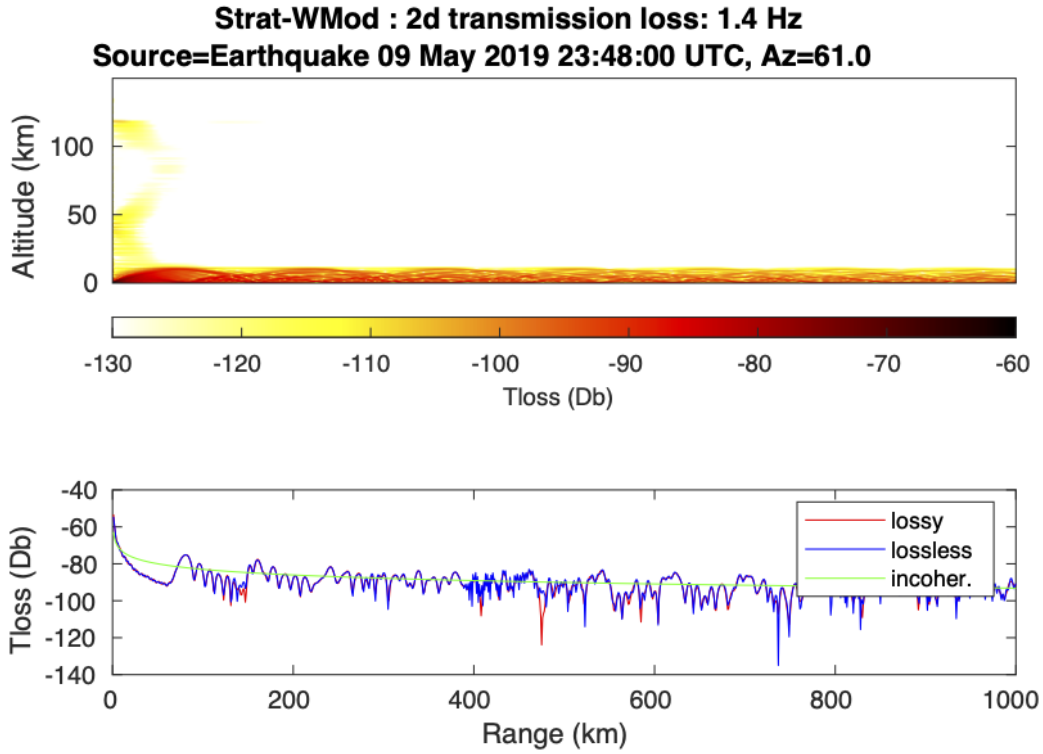
Strat-WMod : 2d transmission loss: 1.4 Hz
Source=Earthquake 09 May 2019 23:48:00 UTC, Az=61.0
Altitude (km)
Tloss (Db)
lossy
lossless
incoher.
Range (km)

Fig. (17): The 1-d and 2-d transmission loss using high order parabolic equation (Pape) and wide angle high mach modal (Wmod) at frequency 1.4 Hz to azimuth 61 degree within range 1000 km.

CONCLUSIONS

1- KUT. Sensors Network usually detected the arrival of P-waves for the stations near the epecntral locations for the earthquakes with ,normal and reverse mechanims.

2- Earthquaskes with magnitudes equal or greater than 5.5 mb can genrate infrasound waves and propgated for long distances

3- The earthquakes recorded on the oceon can generate infarsound waves through the T-phases which can travel to long distances in SOFAR layer and can be detected in hydroacoustic stations.

4- The coupling from the oceon to the air occured in the earthqauke of 09 of May, 2020 (23:48:00 UTC) and well-recorded in I30 , K53 and H11N stations

5-The forward propgataion modeling is neccesary to confirm the infarsound arrivals to the stations

6- AVOG2S model applied to integrate the reanalysis horizontal wind speed data from (NCEP) with numerical wind prediction from (HWM14) to reach to higher altitudes of atmosphere.

7-Ray tracing confirmed of tropospheric arrivals to range 870 km in azimuth direction of I30JP & K53.

8-Transimission loss equation used by two techniques{Range Indpendent Method (using Normal Modess) , Range Dependent Method(using Parapolic Equations)}

9- both propgations methods confirmed the arrival of tropospheric phases with frequancy 1.4 at distance 870 km which is well correlated with result from real data

AUTHOR INFORMATION

I. H. Hamama:

** Ph.D. student at Kochi University of Technology since April 2019.

** Researcher Assistant at National Research Institute of Astronomy and Geophysics, Egyptian National Data Center. **Msc. In Mansoura University, Egypt, (2017) entitled " Analysis of IMS. infrasound data for source verification"

https://orcid.org/0000-0001-9296-412X (https://orcid.org/0000-0001-9296-412X)

E-mail: islam.hamama@nriag.sci.eg

ABSTRACT

Infrasound waves can be defined as the sound waves with frequency range from 0.003 to 20 Hz. Kochi University of Technology (KUT) Infrasound Sensor Network contains 30 infrasound sensors which are distributed all over Japan, a large number of sensors are located in Shikoku Island, all infrasound stations installed with accelerometers to measure the peak ground acceleration (PGA) which can be a good detector for infrasound sources occur on or under the ground like earthquakes.

Many earthquakes detected by our network after establishing of the network since 2016. In this study we will focus on all the possibilities for infrasound detection from earthquakes using KUT sensor network and International Monitoring system (IMS) stations for the earthquakes which were detected in southern of Japan during 2019. The selected events for this study are recorded in different international databases; Reviewed Event Bulletin (REB) database of International Data Center (IDC) , Japan Meteorological Agency (JMA) and United States Geological Survey (USGS). There are different scenarios for infrasound coupling from earthquakes one of these scenarios is the conversion of seismic waves to acoustic from the generated T-phases of oceanic earthquakes. On 09 of May 2019, at 23:48:00 UTC an earthquake with magnitude 6.0 mb happened in west of Kyushu Island and infrasound sensors recorded a clear P-waves, However station K53 and I30JP recorded infrasound waves at distances ranges between 850 to 870 km, In addition to T-phases well-recorded from the earthquake in H11N station near Wake island at 3750 km from the event. Progressive multi-channel cross correlation method applied on both infrasound and hydroacoustic data to identify the arrival phases and the back-azimuth of the waves from station to the source.

Moreover, infrasound propagation simulation applied to the event to confirm the infrasound arrivals. Ground to Space Model (AVO-G2S) used with HWM-14 and NRL-MSISE to construct the atmospheric profile for higher altitudes up to 180 km over the event area,

furthermore the 3d ray tracing process and the calculation of the transmission loss equation by normal modes and parabolic equation methods applied.

In conclusion this study shows the earthquake detectability from infrasound waves using local infrasound sensors for the largest earthquakes occurred in southern of Japan during 2019. Many parameters control the generation of infrasound from earthquakes; magnitude, depth, mechanism and the topographic features. In addition to the T-phases generation through the SOFAR layer can be an evidence of seismic conversion to sound for the oceanic earthquakes as occurred on the earthquake of 09 May 2019, after applying the propagation simulation with (AVO-G2S) model on this earthquake the tropospheric arrivals confirmed and the calculated celerities well-correlated with the real detected data .

REFERENCES

- Mikumo, T., 1968, Atmospheric pressure waves and tectonic deformation

associated with the Alaskan earthquake of March 28, 1964, Journal of Geophysical Research,

https://doi.org/10.1029/JB073i006p02009 (https://doi.org/10.1029/JB073i006p02009)

2- Che, I., Lee, H., Jeon, J. ,2006, An analysis of the infrasound signal from the Miyagi-Oki earthquake in Japan on 16 August 2005. Earth Planet Sp 59, e9–e12 (2007). https://doi.org/10.1186/BF03353092 (https://doi.org/10.1186/BF03353092)

3- Mutschlecner, J. P. and R. W. Whitaker, 2005, Infrasound from earthquakes, J.

Geophys. Res., 110, D01108, https://doi.org/10.1029/2004JD005067 (https://doi.org/10.1029/2004JD005067)

4- Hernandez, B., Le Pichon A., Vergoz J.,Herry P., Ceranna L., Pilger C., Marchetti E., Ripepe M., Bossu R. ,2018, Estimating the Ground−Motion Distribution of the 2016 MwMw 6.2 Amatrice, Italy, Earthquake Using Remote Infrasound Observations. Seismological Research Letters ; 89 (6): 2227–2236. doi: https://doi.org/10.1785/0220180103 (https://doi.org/10.1785/0220180103)

5- Kim, T. S., Hayward, C., and Stump, B. (2004), Local infrasound signals from the Tokachi−Oki earthquake, Geophys. Res. Lett., 31, L20605, doi:10.1029/2004GL021178.

6- Le Pichon, A., Guilbert, J., Vega, A., Garcés, M., and Brachet, N., Ground−coupled air waves and diffracted infrasound from the Arequipa earthquake of June 23, 2001, Geophys. Res. Lett., 29(18), 1886, doi:10.1029/2002GL015052, 2002.

7- Okano K., Kimura S., Seismicity characteristics in shikoku in relation to the great nankaido earthquakes,1979, Journal of Physics of the Earth, Volume 27, issue 5, pages 373-381, https://doi.org/10.4294/jpe1952.27.373.

8- Evers, L. G., Brown, D., Heaney, K. D., Assink, J. D., Smets, P. S. M., and Snellen, M. (2014), Evanescent wave coupling in a geophysical system: Airborne acoustic signals from the M w 8.1 Macquarie Ridge earthquake, Geophys. Res. Lett., 41, 1644–1650, doi:10.1002/2013GL058801.

9- Cansi, Y. (1995) An Automatic Seismic Event Processing for Detection and Location: The P.M.C.C. Method. Geophysical Research Letters, 22, 1021-1024.
https://doi.org/10.1029/95GL00468 (https://doi.org/10.1029/95GL00468)

10- Hans F. Schwaiger, Alexandra M. Iezzi, David Fee,2019,

AVO-G2S: A modified, open-source Ground-to-Space atmospheric specification for infrasound modeling,Computers & Geosciences,Volume 125,Pages 90-97,https://doi.org/10.1016/j.cageo.2018.12.013.

11- Blom, P.S., 2014. GeoAc: numerical tools to model acoustic propagation in the geometric

limit. Software. https://github.com/LANL-Seismoacoustics/GeoAc.

12- Waxler, R.M., Assink, J.D., Hetzer, C., Velea, D., 2017. NCPAprop–a software package for infrasound propagation modeling. J. Acoust. Soc. Am. 141 (5).

13- NCEP Reanalysis Data, 2019. Kalnay et al.,The NCEP/NCAR 40-year reanalysis project, Bull. Amer. Meteor. Soc., 77, 437-470, 1996.

14- Drob, D. P., Emmert, J. T., Meriwether, J. W., Makela, J. J., Doornbos, E., Conde, M., Hernandez, G., Noto, J., Zawdie, K. A., McDonald, S. E., et al. (2015), An update to the Horizontal Wind Model (HWM): The quiet time thermosphere, Earth and Space Science, 2, 301– 319, doi:10.1002/2014EA000089.

15- Picone, J. M., Hedin, A. E., Drob, D. P., and Aikin, A. C., 200,NRLMSISE−00 empirical model of the atmosphere: Statistical comparisons and scientific issues, J. Geophys. Res., 107(A12), 1468, doi:10.1029/2002JA009430,

16- Winkelman, Andrew T.,2015, NCPA propagation code users manual, Master's Project (M.S.) University of Alaska Fairbanks.

17- Batubara, M., Yamamoto, M.-Y.,2020, Infrasound Observations of Atmospheric Disturbances Due to a Sequence of Explosive Eruptions at Mt. Shinmoedake in Japan on March 2018. Remote Sens. 2020, 12, 728.

18- Japan Meteorological Agency (JMA). Monthly Volcanic Activity Report; Tokyo, Japan, 2018. Available

19-Revivewed Event Bulletin, 2019, International Data Center (IDC),Comprehensive Nuclear Ban Treaty Organization (CTBTO).

20- U.S. Geological Survey, 2017, Earthquake Facts and Statistics, accessed January 02, 2019 at URL:https://earthquake.usgs.gov/earthquakes/search/ (https://earthquake.usgs.gov/earthquakes/search/)

21- National Research Institute for Earth Science and Disaster Resilience (2019),
NIED K-NET, KiK-net, National Research Institute for Earth Science and Disaster Resilience,
doi:10.17598/NIED.0004,https://www.fnet.bosai.go.jp/ (https://www.fnet.bosai.go.jp/)

22- de Groot-Hedlin,Catherine D.,2001, Excitation of T-phases by seafloor scattering, The Journal of the Acoustical Society of America, https://doi.org/10.1121/1.1361057 (https://doi.org/10.1121/1.1361057)

23-InfraPy package for infrasound analysis using F-detector ,GitHub,https://github.com/LANL-Seismoacoustics/infrapy.

24- Drob, D. P., Picone, J. M., and Garcés, M. (2003), Global morphology of infrasound propagation, J. Geophys. Res., 108, 4680, doi:10.1029/2002JD003307, D21.

25- Lingevitch J. F., Collins M. D., Dacol D. K., Drob P. D.,2002, A wide angle and high Mach number parabolic equation, The Journal of the Acoustical Society of America, https://doi.org/10.1121/1.1430683 (https://doi.org/10.1121/1.1430683)

26-DTKGPMCC infrasound analysis program, Comprehensive Nuclear Ban Treaty Organization (CTBTO).

27- QGIS Development Team, 2020. QGIS Geographic Information System. Open Source Geospatial Foundation Project. http://qgis.osgeo.org (http://qgis.osgeo.org)

28- GMT 6: Wessel, P., Luis, J. F., Uieda, L., Scharroo, R., Wobbe, F., Smith, W. H. F., & Tian, D. (2019). The Generic Mapping Tools version 6. Geochemistry, Geophysics, Geosystems, 20, 5556–5564. https://doi.org/10.1029/2019GC008515.

29- Pilger, C., Gaebler, P., Ceranna, L., Le Pichon, A., Vergoz, J., Perttu, A., Tailpied, D., and Taisne, B.,2019, Infrasound and seismoacoustic signatures of the 28 September 2018 Sulawesi super-shear earthquake, Nat. Hazards Earth Syst. Sci., 19, 2811–2825, https://doi.org/10.5194/nhess-19-2811-2019.

30- Shelly, D., Beroza, G., Ide, S. et al.,2006, Low-frequency earthquakes in Shikoku, Japan, and their relationship to episodic tremor and slip. Nature 442, 188–191 (2006). https://doi.org/10.1038/nature04931 (https://doi.org/10.1038/nature04931)

31- Yves Cansi, Alexis Le Pichon,2008, Handbook of Signal Processing in Acoustics, Pages 1425-1435.

32- M.N. ElGabry, I.M. Korrat, H.M. Hussein, I.H. Hamama, 2017, Infrasound detection of meteors, NRIAG Journal of Astronomy and Geophysics,https://doi.org/10.1016/j.nrjag.2017.04.004.

33- Garces M., Le Pichon A.,2009, Infrasound from Earthquakes, TsunamisandVolcanoes. In: Meyers R. (eds) Encyclopedia of Complexity and Systems Science. Springer, New York, NY

https://doi.org/10.1007/978-0-387-30440-3_286 (https://doi.org/10.1007/978-0-387-30440-3_286)